Iterative Intercarrier Interference Mitigation for Pilot-Aided OFDM Channel Estimation Based on Channel Linearizations

Ingmar Groh, *Student Member, IEEE*, Christian Gentner, *Member, IEEE*, and Stephan Sand, *Senior Member, IEEE*

***Abstract*—Orthogonal frequency division multiplexing (OFDM) became a popular transmission approach since it suppresses intersymbol interference (ISI) due to large channel delays. However, intercarrier interference (ICI) for high mobility receivers yields corrupted channel estimates for pilot-aided OFDM channel estimation. Thus, this paper presents a novel time-variant channel estimation approach to mitigate this system impairment. We linearize the time-variant channel and determine the expansion point by channel estimates corresponding to the current OFDM symbol, and we get the unknown channel slopes by an iterative data and channel estimation. Our algorithm combines a least squares or a minimum norm channel slope estimation and the detection of the channel paths. It sets any channel path power equal zero once the corresponding power estimate is smaller than a given threshold. Our algorithm exploits the large channel correlations between the cyclic prefix and the successive OFDM symbol optimally. These maximum correlations reason the superiority of ICI mitigation with cyclic prefixes compared to channel slope estimation with adjacent OFDM symbols, which needs at least twice the number of pilot symbols. Additionally, our iterative ICI mitigation reduces noise impairments.**

***Index Terms*—orthogonal frequency division multiplexing, intercarrier interference, Taylor series expansion, iterative time-variant pilot-aided channel estimation**

I. INTRODUCTION

Multi-carrier transmission approaches divide the symbol rate by the number of subcarriers and decrease thereby intersymbol interference (ISI), which appears especially for large channel delays. Orthogonal frequency division multiplexing (OFDM) provides additionally an efficient separation of the subcarriers both on the transmitter and receiver side. Therefore, the terrestrial and handheld digital video broadcasting (DVB-T and DVB-H) standard [1] and wireless high performance local area networks (HIPERLAN2) [2], and third generation partnership project long term evolution (3GPP-LTE) systems [3] which require high data rates are based on OFDM. However, high-mobility OFDM systems also suffer from intercarrier interference (ICI) [4], which even becomes larger for a decreased subcarrier spacing or equivalently an increased number of subcarriers.

The initial approaches dealing with channel linearization [5] to combat ICI impairments only performed satisfactory for mobile radio channels with low delay and Doppler spread. Thus, advanced ICI mitigation algorithms involving higher order channel approximations as well as Lagrangian or Newton polynomials have been designed. Other ICI mitigation algorithms perform a conjugate transmission [6] with a two path algorithm or coherent and differential ICI cancelation [7]. Alternative approaches use minimum mean square error (MMSE) equalization [8] with parallel ICI cancelation [9] or decision feedback equalization for iterative ICI cancelation [8]. However, to obtain a low complexity ICI mitigation, an improved channel linearization [10] yields promising results.

This paper extends the ICI mitigation in [10], which performs a linearization of the time-variant channel. For it, an iterative data and channel slope estimation [11], [12] with the cyclic prefix and a suitable expansion point are required. Like in [10], we get it by channel estimates corresponding to the current OFDM symbol. However, our novel iterative data and channel estimation combines a least squares or a minimum norm channel slope computation and the detection of the channel paths. We need this threshold operation, which sets any channel path power equal zero once the corresponding estimate is smaller than the threshold, to reduce the influence of noise on the channel estimation. Our iterative channel and data estimation works as follows. We construct least squares or minimum norm channel slope estimates based on the cyclic prefix and instantaneous data estimates. Once we have the channel slope estimates corresponding to the next iteration, we get an improved estimate of the data symbols. This procedure needs at most five iterations until the channel slope estimates converge, if we choose the ICI affected data symbols and vanishing channel slopes as initial values. The least squares and the minimum norm approach outperform the initial implementation according to [10] and exploit the highly correlated channels corresponding to the cyclic prefix and successive OFDM symbol far better. Thus, our iterative ICI mitigation based on cyclic prefixes outperforms the channel slope estimation with adjacent OFDM symbols [10] due to the maximum channel correlations. Hence the algorithms in this paper yield a far better ICI mitigation compared to time-variant channel estimation using Slepians' sequences [11], [13]. We reuse the cyclic prefix, which the channel linearization with adjacent OFDM symbols and the time-variant channel estimation based on Slepians' functions simply throw away, and we only need one OFDM symbol. Thus, we obtain a highly efficient and ICI mitigation, where the number of pilot symbols can be kept low. Furthermore, our iterative ICI mitigation reduces transmission errors due to noise.

This contribution is organized as follows. Sec. II introduces the channel model and Secs. III and IV present the considered OFDM system with the corresponding pilot-aided channel estimation. Simulations in Sec. VI show the superiority of our ICI mitigation in Sec. V compared to the initial implementation [10], and Sec. VII draws some conclusions.

This paper assumes the following notation. Small bold letters denote column vectors, while capital bold letters denote matrices. Serifless font is used for random quantities, e. g. , $\boldsymbol{y} \in \mathbb{C}^N$, while font with serifs is used for deterministic quantities, e. g. , $\boldsymbol{y} \in \mathbb{C}^N$. Operator font is used for functions, e. g. , $\mathrm{g}(t)$. The estimation '$\hat{\bullet}$' and the transpose '$(\bullet)^{\mathrm{T}}$' are the most frequently used mathematical operators. The operator $(\boldsymbol{y})_i$ yields the i-th element of a vector $\boldsymbol{y} \in \mathbb{C}^N$, and the operator $(\boldsymbol{Y})_{i,j}$ yields the (i,j)-th element of a matrix $\boldsymbol{Y} \in \mathbb{C}^{M \times N}$.

I. Groh was with the German Aerospace Center (DLR), Institute for Communications and Navigation (KN), D-82234 Wessling, Germany. He is now with Intel Mobile Communications, Department of Concept Engineering, D-01099 Dresden, Germany, E-mail Ingmar.Groh@intel.com. C. Gentner and S. Sand are with the German Aerospace Center (DLR), Institute for Communications and Navigation (KN), D-82234 Wessling, Germany, E-mail {Christian.Gentner,Stephan.Sand}@dlr.de.

978-1-4673-1881-5/12/$31.00 ©2012 IEEE

II. CHANNEL MODEL

This section introduces the channel model for the investigations in this paper. It consists of a time-variant frequency-selective channel impulse response

$$\mathsf{h}\left(\tau,t\right)=\sum_{g=0}^{G}\mathsf{a}_g\left(t\right)\delta\left(\tau-\tau_g\right), \tag{1}$$

where the channel delays $\tau_g = gT_{\mathrm{S}}$ are assumed to be integer multiples of the sampling time T_{S}. The correlation properties of the time-variant Rayleigh processes $\mathsf{a}_g\left(t\right)$ [14], [15] are characterized by a zero-order Bessel function

$$\mathrm{R}_{\mathsf{a}_{\mathrm{g}}(\mathrm{t})}\left(\tau\right)=\mathrm{E}\left[\mathsf{a}_g^*\left(t\right)\mathsf{a}_g\left(t+\tau\right)\right]=a_g^2\mathrm{J}_0\left(2\pi f_{\mathrm{D,max}}\tau\right), \tag{2}$$

where '$*$' denotes the complex conjugate, where '$\mathrm{E}\left[\bullet\right]$' denotes the expectation operator, and where a_g^2 defines the power delay profile (PDP) for $g=0,\ldots,G$.

III. OFDM SYSTEM MODEL

This section describes the OFDM system model, where K OFDM symbols and N subcarriers form one OFDM frame [1] and where the (inverse) fast Fourier transform (IFFT and FFT) converts the time-domain symbols $x_n^{(k)}$ into the modulation symbols $X_i^{(k)}$ at the $i-$th subcarrier for $i=0,\ldots,N-1$ of the $k-$th OFDM symbol for $k=0,\ldots,K-1$ and vice versa. The observation vector at the OFDM receiver reads

$$\boldsymbol{y}_{\mathrm{S}}^{(k)}=\boldsymbol{H}_{\mathrm{S}}^{(k)}\left[\boldsymbol{x}_{\mathrm{G}}^{(k),\mathrm{T}},\boldsymbol{x}_{\mathrm{S}}^{(k),\mathrm{T}}\right]^{\mathrm{T}}+\boldsymbol{n}_{\mathrm{S}}^{(k)}=\tilde{\boldsymbol{H}}_{\mathrm{S,cyc}}^{(k)}\boldsymbol{x}_{\mathrm{S}}^{(k)}+\boldsymbol{n}_{\mathrm{S}}^{(k)}, \tag{3}$$

since at the OFDM transmitter after the IFFT, the $k-$th guard interval vector $\boldsymbol{x}_{\mathrm{G}}^{(k)}=\left[x_{N-G}^{(k)},\ldots,x_{N-1}^{(k)}\right]^{\mathrm{T}}\in\mathbb{C}^G$ is inserted before the $k-$th symbol vector $\boldsymbol{x}_{\mathrm{S}}^{(k)}=\left[x_0^{(k)},\ldots,x_{N-1}^{(k)}\right]^{\mathrm{T}}\in\mathbb{C}^N$. In (3), the noise vector $\boldsymbol{n}_{\mathrm{S}}^{(k)}=\left[n_0^{(k)},\ldots,n_{N-1}^{(k)}\right]^{\mathrm{T}}\in\mathbb{C}^N$ has the same structure as the observation vector $\boldsymbol{y}_{\mathrm{S}}^{(k)}=\left[y_0^{(k)},\ldots,y_{N-1}^{(k)}\right]^{\mathrm{T}}\in\mathbb{C}^N$, and the non-zero elements of the k-th almost Toeplitz channel matrix $\boldsymbol{H}_{\mathrm{S}}^{(k)}\in\mathbb{C}^{N\times(N+G)}$ read

$$(\boldsymbol{H}_{\mathrm{S}}^{(k)})_{i,j}=\mathsf{a}_{G-j+i}((k(N+G)+i)T_{\mathrm{S}}),\ i\le j\le G+i. \tag{4}$$

The insertion of the k-th cyclic prefix according to (3) enables the rearrangement of the k-th almost Toeplitz channel matrix $\boldsymbol{H}_{\mathrm{S}}^{(k)}\in\mathbb{C}^{N\times(N+G)}$ to the $k-$th almost cyclic matrix

$$\begin{aligned}(\tilde{\boldsymbol{H}}_{\mathrm{S,cyc}}^{(k)})_{i,j}=&\mathsf{a}_{(-j+i)\bmod N}((k(N+G)+i)T_{\mathrm{S}}),\\&(-j+i)\bmod N\le G.\end{aligned} \tag{5}$$

The observation corresponding to the k-th cyclic prefix reads for $k=1,\ldots,K-1$

$$\boldsymbol{y}_{\mathrm{G}}^{(k)}=\boldsymbol{H}_{\mathrm{G}}^{(k)}\left[\boldsymbol{x}_{\mathrm{G}}^{(k-1),\mathrm{T}},\boldsymbol{x}_{\mathrm{G}}^{(k),\mathrm{T}}\right]^{\mathrm{T}}+\boldsymbol{n}_{\mathrm{G}}^{(k)}, \tag{6}$$

where the noise vector $\boldsymbol{n}_{\mathrm{G}}^{(k)}=\left[n_{-G}^{(k)},\ldots,n_{-1}^{(k)}\right]^{\mathrm{T}}\in\mathbb{C}^G$ has the same structure as the observation vector $\boldsymbol{y}_{\mathrm{G}}^{(k)}=\left[y_{-G}^{(k)},\ldots,y_{-1}^{(k)}\right]^{\mathrm{T}}\in\mathbb{C}^G$ and where the almost Toeplitz matrix $\boldsymbol{H}_{\mathrm{G}}^{(k)}\in\mathbb{C}^{G\times 2G}$ consists of the non-zero elements

$$(\boldsymbol{H}_{\mathrm{G}}^{(k)})_{i,j}=\mathsf{a}_{G-j+i}((-G+k(N+G)+i)T_{\mathrm{S}}),\ i\le j\le G+i. \tag{7}$$

For the first OFDM symbol $k=0$, the observation vector reads

$$\boldsymbol{y}_{\mathrm{G}}^{(0)}=\boldsymbol{H}_{\mathrm{G}}^{(0)}\boldsymbol{x}_{\mathrm{G}}^{(0)}+\boldsymbol{n}_{\mathrm{G}}^{(0)}, \tag{8}$$

where the noise vector $\boldsymbol{n}_{\mathrm{G}}^{(0)}$ and the observation vector $\boldsymbol{y}_{\mathrm{G}}^{(0)}$ have the structure according to (6) and where the channel matrix $\boldsymbol{H}_{\mathrm{G}}^{(0)}\in\mathbb{C}^{G\times G}$ is lower triangular

$$(\boldsymbol{H}_{\mathrm{G}}^{(0)})_{i,j}=\mathsf{a}_{-j+i}((-G+i)T_{\mathrm{S}}),\ i\le j. \tag{9}$$

The application of the FFT to the observation vector in (3) yields the frequency-domain observation vector

$$Y_i^{(k)}=H_{i,0}^{(k)}X_i^{(k)}+\underbrace{\sum_{d=1}^{N-1}H_{i,d}^{(k)}X_{(i-d)\bmod N}^{(k)}}_{=I_i^{(k)}}+N_i^{(k)} \tag{10}$$

with the frequency-domain channel

$$\begin{aligned}H_{i,d}^{(k)}=\frac{1}{N}\sum_{g=0}^{G}\sum_{n=0}^{N-1}\mathsf{a}_g\left((k(N+G)+n)T_{\mathrm{S}}\right)\exp\left(-\frac{\mathrm{j}2\pi nd}{N}\right)\\\exp\left(-\frac{\mathrm{j}2\pi g(i-d)}{N}\right)\end{aligned} \tag{11}$$

and the frequency-domain noise

$$N_i^{(k)}=\frac{1}{\sqrt{N}}\sum_{n=0}^{N-1}n_n^{(k)}\exp\left(-\frac{\mathrm{j}2\pi ni}{N}\right), \tag{12}$$

and the ICI $I_i^{(k)}$. For $d=0$, the frequency-domain channel in (11) reads

$$H_{i,0}^{(k)}=\sum_{g=0}^{G}\underbrace{\frac{1}{N}\sum_{n=0}^{N-1}\mathsf{a}_g\left((k(N+G)+n)T_{\mathrm{S}}\right)}_{=\bar{a}_g^{(k)}}\exp\left(-\frac{\mathrm{j}2\pi gi}{N}\right) \tag{13}$$

with the time-averaged channel estimate $\bar{a}_g^{(k)}$.

IV. PILOT-AIDED CHANNEL ESTIMATION IN OFDM SYSTEMS

This section briefly reviews the pilot-aided OFDM channel estimation from the contribution [10]. For any pilot subcarrier $\ell_i=i(N/L),\ i=0,\ldots,L-1$ endowed with time-invariant pilot symbols $X_{\ell_i}^{(k)}=P_{\ell_i}$ [2], the frequency-domain observation vector in (10) yields the frequency-domain channel estimates

$$\hat{H}_{\ell_i,0}^{(k)}=\frac{Y_{\ell_i}^{(k)}}{P_{\ell_i}}=H_{\ell_i,0}^{(k)}+\frac{I_{\ell_i}^{(k)}+N_{\ell_i}^{(k)}}{P_{\ell_i}}, \tag{14}$$

and a successive IFFT yields the time-domain channel estimates

$$\hat{\bar{a}}_g^{(k)}=\frac{1}{L}\sum_{i=0}^{L-1}\hat{H}_{\ell_i,0}^{(k)}\exp\left(\frac{\mathrm{j}2\pi gi}{L}\right),\ g=0,\ldots,G. \tag{15}$$

For moving receivers with $f_{\mathrm{D,max}}>0$, the ICI $I_{\ell_i}^{(k)}$ corrupts the frequency-domain channel estimates $\hat{H}_{\ell_i,0}^{(k)}$ in (14) and thus also the time-domain channel estimates $\hat{\bar{a}}_g^{(k)}$ in (15). To erase estimated channel paths with a power smaller than the maximum channel power in the $k-$th OFDM

symbol $\max_{g=0,\ldots,G}\left|\hat{\bar{a}}_g^{(k)}\right|^2/a_{\text{level}}^2$ corresponding to a level value a_{level}, the time-domain channel estimates $\hat{\bar{a}}_g^{(k)}$ in (15) are postprocessed by a threshold operation [10], which sets $\hat{\bar{a}}_g^{(k)}=0$ for $\left|\hat{\bar{a}}_g^{(k)}\right|<\max_{g=0,\ldots,G}\left|\hat{\bar{a}}_g^{(k)}\right|/a_{\text{level}}$. Also, it yields the number of non-zero channel amplitudes, which decreases the receiver complexity [10] and offers different options for ICI mitigation in the next section.

V. ICI MITIGATION IN OFDM SYSTEMS USING CYCLIC PREFIXES

This section presents our ICI mitigation approach based on cyclic prefixes and a least squares or a minimum norm channel slope estimation. First, we briefly describe the ICI mitigation based on cyclic prefixes, where an accurate estimation of the channel slopes is crucial. Second, to get the channel slope estimates, we present a least squares and a minimum norm channel slope estimation. Third, we summarize the iterative ICI mitigation based on cyclic prefixes including the enhanced channel slope estimation.

We start with an approximation of the time-variant Rayleigh processes $\mathsf{a}_g(t),\ g=0,\ldots,G$ by a linear Taylor series [10]

$$\mathsf{a}_g(t)\approx\mathsf{a}_g(t_0)+m_g(t-t_0) \tag{16}$$

with the channel slopes $m_g=\mathrm{d}\mathsf{a}_g(t_0)/\mathrm{d}t_0$ and the expansion point t_0. For the $k-$th OFDM symbol, we set $t_0^{(k)}=(N/2-1+k(N+G))T_{\text{S}}$ and $t=k(N+G)T_{\text{S}},\ldots,(N-1+k(N+G))\,T_{\text{S}}$ and resort to the time-domain channel estimate $\hat{\bar{a}}_g^{(k)}$ in (15). Thus, the sampling of the linearized Rayleigh processes in (16) yields

$$\hat{\boldsymbol{a}}_{\text{S},g}^{(k)}\approx\hat{\bar{a}}_g^{(k)}\boldsymbol{e}^{(N)}+\hat{m}_g^{(k)}\boldsymbol{t}_{\text{S}} \tag{17}$$

with the sampled Rayleigh processes $\boldsymbol{a}_{\text{S},g}^{(k)}=[\mathsf{a}_g((N+G)kT_{\text{S}}),\ldots,\mathsf{a}_g((k(N+G)+N-1)T_{\text{S}})]^{\text{T}}\in\mathbb{C}^N$ and with the time sample vector $\boldsymbol{t}_{\text{S}}=[1-N/2,\ldots,N/2]^{\text{T}}\in\mathbb{C}^N$, and where $\boldsymbol{e}^{(N)}\in\mathbb{C}^N$ denotes the N-dimensional column vector with one elements. If we plug in the sampled Rayleigh processes in (17) into the frequency-domain channel in (11), we get the frequency-domain channel for $d=0$

$$\hat{H}_{i,0}^{(k)}=\sum_{g=0}^{G}\left(\hat{\bar{a}}_g^{(k)}+\frac{T_{\text{S}}}{2}\hat{m}_g^{(k)}\right)\exp\left(-\frac{\mathrm{j}2\pi gi}{N}\right), \tag{18}$$

and for $d=1,\ldots,N-1$

$$\hat{H}_{i,d}^{(k)}=-\frac{T_{\text{S}}}{1-\exp\left(-\frac{\mathrm{j}2\pi d}{N}\right)}\sum_{g=0}^{G}\hat{m}_g^{(k)}\exp\left(-\frac{\mathrm{j}2\pi g\,(i-d)}{N}\right). \tag{19}$$

For the k-th cyclic prefix, the linearized and sampled Rayleigh processes are

$$\hat{\boldsymbol{a}}_{\text{G},g}^{(k)}\approx\hat{\bar{a}}_g^{(k)}\boldsymbol{e}^{(G)}+\hat{m}_g^{(k)}\boldsymbol{t}_{\text{G}} \tag{20}$$

with the sampled Rayleigh processes $\boldsymbol{a}_{\text{G},g}^{(k)}=[\mathsf{a}_g(((N+G)k-G)T_{\text{S}}),\ldots,\mathsf{a}_g((k(N+G)-1)T_{\text{S}})]^{\text{T}}\in\mathbb{C}^G$, with the time sample vector $\boldsymbol{t}_{\text{G}}=[-G+1-N/2,\ldots,-N/2]^{\text{T}}\in\mathbb{C}^G$, and where $\boldsymbol{e}^{(N)}\in\mathbb{C}^N$ denotes the N-dimensional column vector with one elements. In the next step, we insert the linearized and sampled Rayleigh processes for the k-th cyclic prefix in (20) into the observation vector in (6) to get

$$\boldsymbol{y}_{\text{G}}^{(k)}-\bar{\boldsymbol{H}}_{\text{G}}^{(k)}\left[\boldsymbol{x}_{\text{G}}^{(k-1),\text{T}},\boldsymbol{x}_{\text{G}}^{(k),\text{T}}\right]^{\text{T}}=T_{\text{S}}\,\text{diag}\left\{\boldsymbol{t}_{\text{G}}\right\}\boldsymbol{X}_{\text{G}}^{(k)}\hat{\boldsymbol{m}}^{(k)} \tag{21}$$

with the diagonal matrix $\text{diag}\left\{\boldsymbol{t}_{\text{G}}\right\}$ with the elements of the vector $\boldsymbol{t}_{\text{G}}$ on its diagonal, with the channel slope vector $\boldsymbol{m}^{(k)}=\left[m_0^{(k)},\ldots,m_G^{(k)}\right]^{\text{T}}\in\mathbb{C}^{G+1}$, with the Toeplitz channel matrix $\bar{\boldsymbol{H}}_{\text{G}}^{(k)}\in\mathbb{C}^{G\times 2G}$ with the elements

$$(\bar{\boldsymbol{H}}_{\text{G}}^{(k)})_{i,j}=\hat{\bar{a}}_{G-j+i}^{(k)},\ i\le j\le G+i, \tag{22}$$

and with the Toeplitz symbol matrix $\boldsymbol{X}_{\text{G}}^{(k)}\in\mathbb{C}^{G\times G+1}$ with the elements

$$\left(\boldsymbol{X}_{\text{G}}^{(k)}\right)_{i,j}=\left(\left[\boldsymbol{x}_{\text{G}}^{(k-1),\text{T}},\boldsymbol{x}_{\text{G}}^{(k),\text{T}}\right]^{\text{T}}\right)_{G+1+i-j}. \tag{23}$$

We now present our two fundamental original contributions which allow an improvement of the ICI mitigation based on cyclic prefixes. The first solution $\hat{\boldsymbol{m}}_{\text{LS}}^{(k)}$ requires the set

$$\mathcal{G}=\left\{g:\left|\hat{\bar{a}}_g^{(k)}\right|\ge\max_{g=0,\ldots,G}\left|\hat{\bar{a}}_g^{(k)}\right|/a_{\text{level}}\right\}, \tag{24}$$

and its complementary set

$$\bar{\mathcal{G}}=\{0,\ldots,G\}\setminus\mathcal{G} \tag{25}$$

to define $\left(\hat{\boldsymbol{m}}_{\text{LS}}^{(k)}\right)_{\bar{\mathcal{G}}}=0$ and to perform a least squares approach for the channel slope vector $\left(\hat{\boldsymbol{m}}_{\text{LS}}^{(k)}\right)_{\mathcal{G}}$ based on $\boldsymbol{y}_{\text{G}}^{(k)}-\bar{\boldsymbol{H}}_{\text{G}}^{(k)}\left[\boldsymbol{x}_{\text{G}}^{(k-1),\text{T}},\boldsymbol{x}_{\text{G}}^{(k),\text{T}}\right]^{\text{T}}$ and the columns of $T_{\text{S}}\,\text{diag}\left\{\boldsymbol{t}_{\text{G}}\right\}\boldsymbol{X}_{\text{G}}^{(k)}\in\mathbb{C}^{G\times G+1}$ corresponding to set $\mathcal{G}$. As a second channel slope estimation, we solve the optimization problem

$$\hat{\boldsymbol{m}}_{\text{MN}}^{(k)}=\underset{\hat{\boldsymbol{m}}^{(k)}}{\text{argmin}}\left\|\hat{\boldsymbol{m}}^{(k)}\right\|_2^2\,\text{s.t. (21)}, \tag{26}$$

where the operator 'argmin' yields the input that minimizes the cost function subject to (s.t.) the observation in (21), by the right-hand inverse of $T_{\text{S}}\,\text{diag}\left\{\boldsymbol{t}_{\text{G}}\right\}\boldsymbol{X}_{\text{G}}^{(k)}\in\mathbb{C}^{G\times G+1}$ and $\boldsymbol{y}_{\text{G}}^{(k)}-\bar{\boldsymbol{H}}_{\text{G}}^{(k)}\left[\boldsymbol{x}_{\text{G}}^{(k-1),\text{T}},\boldsymbol{x}_{\text{G}}^{(k),\text{T}}\right]^{\text{T}}\in\mathbb{C}^G$. Afterwards, we perform the threshold operation according to Sec. IV, i. e. , we set $\left(\hat{\boldsymbol{m}}_{\text{MN}}^{(k)}\right)_{g+1}=0$ for $\left|\hat{\bar{a}}_g^{(k)}\right|<\max_{g=0,\ldots,G}\left|\hat{\bar{a}}_g^{(k)}\right|/a_{\text{level}}$. The processing of the first OFDM symbol for $k=0$ in (8) yields $\boldsymbol{x}_{\text{G}}^{(-1)}=\boldsymbol{0}_G$. Thus, the matrix $\boldsymbol{X}_{\text{G}}^{(k)}\in\mathbb{C}^{G\times G+1}$ becomes a lower triangular matrix with zeros on its diagonal. Thus, the minimum norm approach for channel slope computation is prohibitive and we need to choose the least squares implementation. Contrary, for OFDM symbols with $k\ge 1$, only the minimum norm method in (26) removes all interferences between different channel slopes. Only for $k=0$ and $\boldsymbol{x}_{\text{G}}^{(-1)}=\boldsymbol{0}_G$, the interferences between different channel slopes in the matrix vector product $\bar{\boldsymbol{H}}_{\text{G}}^{(k)}\left[\boldsymbol{x}_{\text{G}}^{(k-1),\text{T}},\boldsymbol{x}_{\text{G}}^{(k),\text{T}}\right]^{\text{T}}$ in (21) are sufficiently small to obtain a good least squares estimation.

The iterative ICI mitigation works as follows [10]. We set $\boldsymbol{x}_{\text{G}}^{(-1)}=\boldsymbol{0}_G$ or we assume $\boldsymbol{x}_{\text{G}}^{(k-1)}$, $k\ge 1$ to be known at the receiver. An initial estimate for $\hat{\boldsymbol{x}}_{\text{G}}^{(k)}$ and $\hat{\boldsymbol{X}}_{\text{G}}^{(k)}$ corresponding

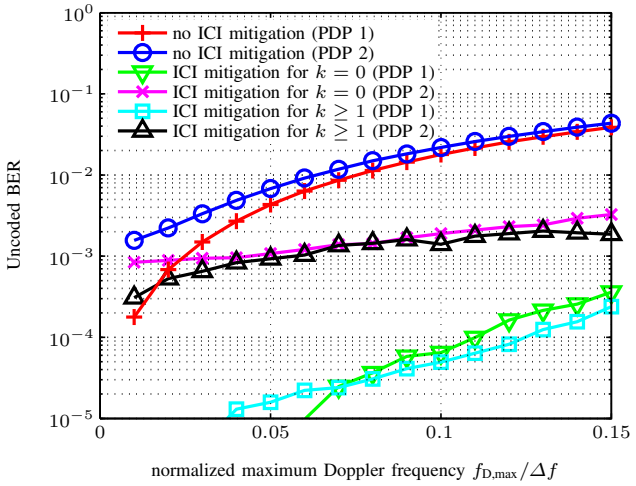

Figure 1. Uncoded BERs versus the normalized maximum Doppler frequency $f_{\mathrm{D,max}}$ with and without ICI mitigation for PDP 1 and 2. For $k = 0$, we use the least squares channel slope estimation, while for $k \geq 1$, we use the minimum norm channel slope estimation.

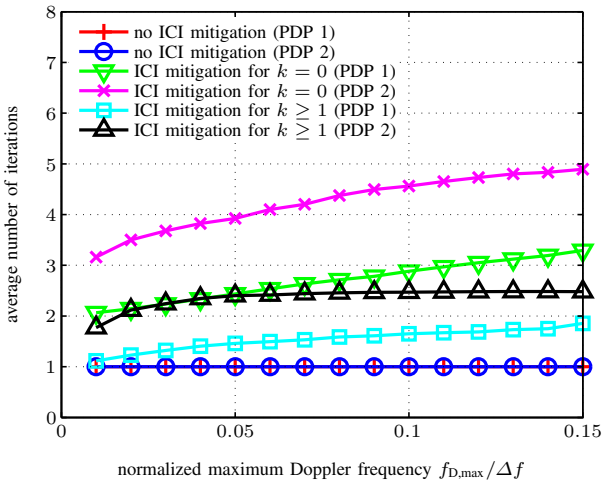

Figure 2. Average number of iterations versus the normalized maximum Doppler frequency $f_{\mathrm{D,max}}$ with and without ICI mitigation for PDP 1 and 2. For $k = 0$, we use the least squares channel slope estimation, while for $k \geq 1$, we use the minimum norm channel slope estimation.

to $\hat{\boldsymbol{m}}_{\mathrm{MN}}^{(k)} = \hat{\boldsymbol{m}}_{\mathrm{LS}}^{(k)} = \mathbf{0}_{G+1} \in \mathbb{C}^{G+1}$ is obtained by the frequency-domain channel in (18) and (19), and a zero-forcing estimation of the data symbols $\hat{X}_i^{(k)}$ in (10) followed by an IFFT. We get the next channel slope estimates $\hat{\boldsymbol{m}}_{\mathrm{MN}}^{(k)}$ or $\hat{\boldsymbol{m}}_{\mathrm{LS}}^{(k)}$ by resolving (21) with the minimum norm or with the least squares method. Again, the next time-domain data symbol estimates for $\hat{\boldsymbol{x}}_{\mathrm{G}}^{(k)}$ and $\hat{\boldsymbol{X}}_{\mathrm{G}}^{(k)}$ are computed by (18), (19), and (10) and a successive IFFT. We repeat the iterations until the channel slopes $\hat{\boldsymbol{m}}_{\mathrm{MN}}^{(k)}$ or $\hat{\boldsymbol{m}}_{\mathrm{LS}}^{(k)}$ converge or the fifth iteration is reached, although two to three iterations usually suffice.

VI. SIMULATIONS AND RESULTS

We consider with PDP 1 and 2 according to [10] two single frequency network channels to show the superiority of our ICI mitigation in Sec. V, and also all system parameters are the same as in [10]. For all simulations in this section, we assume the level value $a_{\mathrm{level}} = 10$ [10] for the threshold operation in Secs. IV and V, to obtain an efficient noise and interference reduction and an accurate channel estimation. Figs. 1 and 2 consider a vanishing noise intensity and various Doppler spreads, while Figs. 3 and 4 consider various signal to noise ratios (SNRs) and a Doppler spread of $f_{\mathrm{D,max}}/\Delta f = 0.065$.

Figs. 1 and 2 summarize the simulations for PDP 1 and 2 and different normalized maximum Doppler frequencies $f_{\mathrm{D,max}}/\Delta f$. In Fig. 1, we observe a smaller bit error ratio (BER) for PDP 1 compared to PDP 2 because of the smaller delay spread. This BER difference vanishes for an increasing Doppler spread, which increases the ICI. We observe for both PDPs a substantial BER reduction for the channel linearization based ICI mitigation. The comparison of Fig. 1 with the previous implementation in [10] reveals that the modified channel slope estimation in Sec. V exploits the time correlations optimally. We compare the BERs of our cyclic prefix based ICI mitigation results in Fig. 1 and [10] and see the advances of the estimation algorithm in Sec. V. Our algorithm applied to PDP 1 reduces for $f_{\mathrm{D,max}}/\Delta f = 0.1$ the BER from $2 \cdot 10^{-3}$ to values below 10^{-4}. This performance gain holds for PDP 2 as well, where the minimum norm and least squares channel slope estimation reduce the BER from $6 \cdot 10^{-3}$ for $f_{\mathrm{D,max}}/\Delta f = 0.1$ to values below $2 \cdot 10^{-3}$. The large channel correlations between the cyclic prefix and the OFDM symbol also guarantee a convergence of the iterative data and channel estimation throughout the considered Doppler range. Since the time difference between any cyclic prefix and its successive OFDM symbol is always smaller than that between several OFDM symbols which are separated by the guard time, any channel slope computation by adjacent OFDM symbols [10] yields inferior BER results. The BER reduction holds for the least squares and minimum norm algorithm, but especially for large Doppler spreads, the BER corresponding to the minimum norm approach is smaller than that of the least squares algorithm. Fig. 2 investigates the convergence performance of the iterative data and channel slope estimation. We see for both PDPs and both cyclic prefixes a fast convergence after only few iterations. We have for PDP 1 always fewer iterations compared to PDP 2 due to the smaller delay spread. Also, the minimum norm slope computation always converges faster than the least squares method. Figs. 1 and 2 assume for the minimum norm slope estimation a perfect knowledge of the preceding OFDM symbol.

Figs. 3 and 4 consider the BERs and the convergence for a fixed maximum Doppler frequency $f_{\mathrm{D,max}}/\Delta f = 0.065$ for different SNRs. Even in the SNR range between 10 dB and 15 dB, the BERs are improved by our iterative ICI mitigation since both the least squares and the minimum norm slope estimation reduce the noise impairments [11]. Evidently, a channel slope estimation based on adjacent OFDM symbols without iterations [10] cannot yield this advantage. The uncorrelated noise causes convergence problems for PDP 2 since the iterative solution of the nonlinear system in Sec. V contains too many degrees of freedom. These difficulties do not arise for PDP 1 which only requires the estimation of two slopes. For high SNRs, we get rid of convergence problems for both PDPs and the BER improvements of our ICI mitigation algorithms become clear. Likewise as in Fig. 1, the performance gain of ICI mitigation for PDP 1 is larger due to the smaller delay spread. The BER curves without ICI mitigation saturate at about 10^{-2}, and for PDP 1 the BER saturation is reduced below 10^{-4}. Contrary, the BER saturation for PDP 2 with the larger delay spread is about

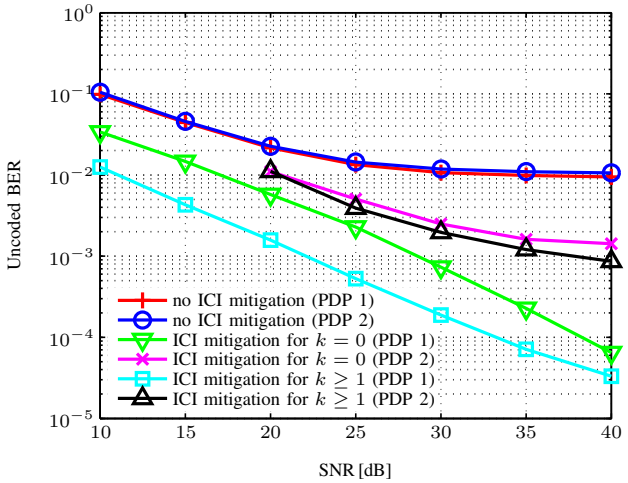

Figure 3. Uncoded BERs versus the SNR with and without ICI mitigation for the normalized maximum Doppler frequency $f_{\mathrm{D,max}}/\Delta f = 0.065$ for PDP 1 and 2. For $k = 0$, we use the least squares channel slope estimation, while for $k \geq 1$, we use the minimum norm channel slope estimation. Note that for PDP 2, our ICI mitigation converges only for SNRs above or equal 20 dB.

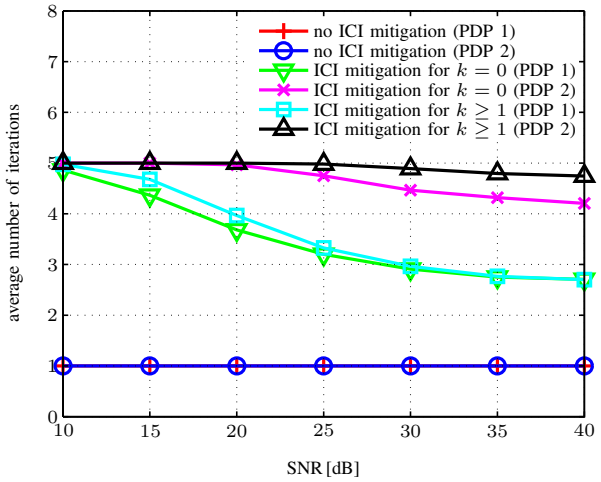

Figure 4. Average number of iterations versus the SNR with and without ICI mitigation for the normalized maximum Doppler frequency $f_{\mathrm{D,max}}/\Delta f = 0.065$ for PDP 1 and 2. For $k = 0$, we use the least squares channel slope estimation, while for $k \geq 1$, we use the minimum norm channel slope estimation.

one order of magnitude larger than for PDP 1. For any SNR between 10 dB and 40 dB, the minimum norm channel slope approach yields a smaller BER than the least squares channel slope computation for the initial OFDM symbol. The BER comparison in Fig. 3 of our cyclic prefix based ICI mitigation and of [10] yields that our methods outperform the former implementation by far. We observe for the ICI mitigation for PDP 1 and 2 according to [10] BERs of $4 \cdot 10^{-3}$ and $8 \cdot 10^{-3}$ at an SNR of 25 dB, while Fig. 3 shows the improved BERs as $5 \cdot 10^{-4}$ and $2 \cdot 10^{-3}$ for PDP 1 and $4 \cdot 10^{-3}$ and $5 \cdot 10^{-3}$ for PDP 2. The minimum time distances between the guard interval and its OFDM symbol induce maximum channel correlations, which our method exploits. However, for large delay spreads and low SNR, we must estimate the slopes with adjacent OFDM symbols since the algorithms fail to converge. Fig. 4 shows again for the noisy scenario a faster convergence for PDP 1 compared to PDP 2. Both PDPs require an increased number of iterations for decreased SNR.

VII. CONCLUSIONS

This paper presents a novel ICI mitigation method for OFDM channel estimation. Simulations reveal that the processing of the ICI impaired channel estimates yields a poor system performance especially for high mobility receivers. Our key enhancement of the ICI mitigation based on cyclic prefixes, which most OFDM receiver algorithms discard, consists in the sophisticated channel slope estimation. We combine the least squares or minimum norm slope estimation with a noise and interference threshold that keeps the number of relevant channel paths low. Our iterative channel slope and data detection reduces the ICI especially for large Doppler spreads and high noise intensities. Additionally, our results show the superiority of our iterative time-variant channel estimation compared to the channel linearization with adjacent OFDM symbols, which even needs twice or three times the number of pilots. The improved BER is due to a maximum channel correlation of the cyclic prefix and the successive OFDM symbol that our method exploits.

REFERENCES

[1] *ETSI EN 300 744 V1.5.1, European Standard (Telecommunications Series) Digital Video Broadcasting (DVB); Framing Structure, Channel Coding and Modulation for Digital Terrestrial Television*, November 2004.

[2] *ETSI TS 101 475 V1.3.1, Technical Specification Broadband Radio Access Networks (BRAN); HIPERLAN Type 2; Physical (PHY) Layer*, December 2001.

[3] 3GPP TS 36.211, *Envolved Universal Terrestrial Radio Access (E-UTRA) - Physical Channels and Modulation, V9.1.0*, http://www.3gpp.org, April 2010.

[4] L. Rugini and P. Banelli, "BER of OFDM Systems Impaired by Carrier Frequency Offset in Multipath Fading Channels," *IEEE Transactions on Wireless Communications*, vol. 4, no. 5, pp. 2279–2288, September 2005.

[5] W. G. Jeon, K. H. Chang, and Y. S. Cho, "An Equalization Technique for Orthogonal Frequency-Division Multiplexing Systems in Time-Variant Multipath Channels," *IEEE Transactions on Communications*, vol. 47, no. 1, pp. 27–32, January 1999.

[6] H.-G. Yeh, Y.-K. Chang, and B. Hassibi, "A Scheme for Cancelling Intercarrier Interference Using Conjugate Transmission in Multicarrier Communication systems," *IEEE Transactions on Wireless Communications*, vol. 6, no. 1, pp. 3–7, January 2007.

[7] S. Lu and N. Al-Dhahir, "Coherent and Differential ICI Cancellation for Mobile OFDM with Application to DVB-H," *IEEE Transactions on Wireless Communications*, vol. 7, no. 11, pp. 4110–4116, November 2008.

[8] R. Merched, "Fast Algorithms in Slow and High Doppler Mobile Environments," *IEEE Transactions on Wireless Communications*, vol. 9, no. 9, pp. 2890–2901, September 2010.

[9] W.-S. Hou and B.-S. Chen, "ICI Cancellation for OFDM Communication Systems in Time-Varying Multipath Fading Channels," *IEEE Transactions on Wireless Communications*, vol. 4, no. 5, pp. 2100–2110, September 2005.

[10] Y. Mostofi and D. C. Cox, "ICI Mitigation for Pilot-Aided OFDM Mobile Systems," *IEEE Transactions on Wireless Communications*, vol. 4, no. 2, pp. 765–774, March 2005.

[11] T. Zemen, C. F. Mecklenbräuker, J. Wehinger, and R. R. Müller, "Iterative Joint Time-Variant Channel Estimation and Multi-User Detection for MC-CDMA," *IEEE Transactions on Wireless Communications*, vol. 5, no. 6, pp. 1469–1478, June 2006.

[12] A. Molisch, M. Toeltsch, and S. Vermani, "Iterative Methods for Cancellation of Intercarrier Interference in OFDM Systems," *IEEE Transactions on Vehicular Technology*, vol. 56, no. 4, pp. 2158–2167, July 2007.

[13] T. Zemen and C. F. Mecklenbräuker, "Time-Variant Channel Estimation Using Discrete Prolate Spheroidal Sequences," *IEEE Transactions on Signal Processing*, vol. 53, no. 9, pp. 3597–3607, September 2005.

[14] W. C. Jakes, *Microwave Mobile Communications*, John Wiley, IEEE Press, New York, USA, 1994.

[15] H. Meyr, M. Moeneclaey, and S. A. Fechtel, *Digital Communication Receivers*, John Wiley, New York, USA, 1997.